



ELSEVIER

Available online at [www.sciencedirect.com](http://www.sciencedirect.com)

SCIENCE @ DIRECT®

Nuclear Instruments and Methods in Physics Research A 499 (2003) 66–74

**NUCLEAR  
INSTRUMENTS  
& METHODS  
IN PHYSICS  
RESEARCH**  
Section A[www.elsevier.com/locate/nima](http://www.elsevier.com/locate/nima)

## The vacuum system of KEKB

K. Kanazawa\*, S. Kato, Y. Suetsugu, H. Hisamatsu, M. Shimamoto, M. Shirai

*High Energy Accelerator Research Organization, 1-1 Oho, Tsukuba, Ibaraki 305-0801, Japan*

Received 18 December 2001; received in revised form 15 May 2002; accepted 1 June 2002

### Abstract

For the KEK B-factory, two rings with a circumference of 3016 m, mainly made of copper, were constructed. A gap between the flanges is filled using Helicoflex as a vacuum seal. The contact force of an RF finger in a bellows is assured by using a spring finger. Pumping slots are backed by crossing bars to prevent the penetration of beam-induced fields. To obtain a pressure of  $10^{-9}$  Torr with the beam when the photo-desorption coefficient reaches  $10^{-6}$ , the design of pump layout is aimed to realize  $100 \ell \text{ s}^{-1} \text{ m}^{-1}$ . NEG strips are used as the main pump. Chemical polishing is applied to clean the extruded surface of a copper chamber. Almost all chambers were baked before installation. Only ion pumps were baked in situ. The photo-desorption coefficient at the start of commissioning was slightly higher than expected, but a decrease of the coefficient is as expected on the whole. At high currents, some bellows were found to be warmed by the TE mode of beam induced fields. The effect of the electron cloud became evident, especially in the LER. Direct damage by the beam is seen at the surface of the movable mask.

© 2002 Elsevier Science B.V. All rights reserved.

PACS: 29.20

Keywords: Accelerator; Electron storage ring; Copper; Photon desorption; Electron cloud; Beam damage

### 1. Introduction

The collider of KEKB consists of two rings which intersect at IR. They are placed side by side in the tunnel. The B-factory is characterized by parameters to obtain a high luminosity. The design current is much higher than that of the existing synchrotron light sources. The vacuum system for the B-factory rings must deal with the synchrotron radiation emitted by very high-current beams, which causes a high gas load and deposits intense

heat in the beam duct (Table 1). The bunch length is designed to be so short (4 mm) that a circulating beam current has a wide range of the frequency spectrum. It is important how to bridge or shield such structures as a flange gap, an aperture for pumping and especially a bellows, so as not to trap a beam induced field or not to cause heat-up of the vacuum components.

The commissioning of KEKB started December, 1998. During the early commissioning, the performance of the vacuum system was satisfactory. Before July, 2001, a fill with an initial current of 940 mA positrons and 730 mA electron was established and the world-record luminosity was achieved. With increasing the current, some

\*Corresponding author. Tel.: +81-298-64-5252; fax: +81-298-64-3182.

E-mail address: [ken-ichi.kanazawa@kek.jp](mailto:ken-ichi.kanazawa@kek.jp) (K. Kanazawa).

Table 1  
Machine parameters concerning the heat-load on the vacuum components

	LER (Positron)	HER (Electron)	Unit
Beam energy	3.5	8.0	GeV
Beam current	2.6	1.1	A
Circumference	3016	←	m
Bending radius	16.31	104.46	m
Total power of SR	2117 (arc)	3817	kW
Critical energy of SR	5.84	10.9	keV
Total photon flux of SR	$7.35 \times 10^{21}$	$7.11 \times 10^{21}$	photons s <sup>-1</sup>
Local maximum of the linear power density	14.8 (bend) ~10 (wiggler)	5.8 (bend)	kW m <sup>-1</sup>
Average linear photon density	$3.3 \times 10^{18}$	$3.2 \times 10^{18}$	photons s <sup>-1</sup> m <sup>-1</sup>

unexpected phenomena appeared. The most serious problem of the vacuum hardware was seen for movable masks. The most serious phenomenon related to the vacuum system is the electron cloud instability in the low energy ring (LER).

This paper covers the main features of the vacuum design [1,2] and some topics related to the vacuum system. Special vacuum chambers, such as cavities and feedback hardware, are not included. IR vacuum chambers are described elsewhere. The story of the movable mask is reported separately.

## 2. Vacuum design

### 2.1. Beam duct

The standard aperture of the LER is a circle with a diameter of 94 mm. For the injection straight with kicker magnets, the aperture is reduced to a racetrack of 76 mm × 48 mm. At the two-level crossing of the rings, the diameter of the LER aperture is 64 mm. Pick-up electrodes for the feedback control are also installed in a duct with a diameter of 64 mm. At the region within 100 m from IP, which is used to correct the chromaticity locally, the aperture is widened to a racetrack of 150 mm × 94 mm. The high energy ring (HER) has a standard aperture of a racetrack of 104 mm × 50 mm. The aperture of the injection straight of the HER is a smaller racetrack of 65 mm × 48 mm. Near IR, the standard aperture

is horizontally enlarged to 150 mm × 50 mm. Near RF cavities, the aperture of both rings is 150 mm in diameter. The beam ducts of both rings have no antechambers.

Most vacuum chambers are made of copper. Copper's high thermal conductivity gives a tolerable temperature gradient for the high peak heat load. In addition, copper works as a shield against radiation from the beam [3]. The grade of copper is ASM C10100 (oxygen-free electronic copper) for a vacuum surface, and C10200 (oxygen-free copper) elsewhere. The beam duct is made by cold forming from an extruded pipe. The pipe wall is 6 mm thick. With this thickness, synchrotron radiation yields a radiation dose of less than 10<sup>5</sup> and 10<sup>7</sup> rad y<sup>-1</sup> outside of a beam duct for the LER and the HER, respectively, running 200 days per year with the design current [4]. In the LER, the maximum heat deposit on the duct wall reaches 14.8 kW m<sup>-1</sup>. The temperature by the heat is estimated to be 120°C, and a strain of -0.15% is induced. This part of the wall receives a heat cycle according to the change in the stored current. In a laboratory fatigue experiment, with the strain changing from 0 to 0.3 at an elevated temperature of 150–200°C, the copper test piece shows no significant decrease of stress up to 10<sup>4</sup> cycle [5]. This result shows that the condition of the beam duct is not critical.

Vacuum flanges are made of stainless steel AISI304. The magnetic permeability of stainless steel is specified to be less than 1.2 so as not to magnetically disturb the beam.

## 2.2. Vacuum surface characterization

In an electron storage ring, the main outgassing with a beam is due to desorption by synchrotron radiation. The amount of desorption is proportional to the number of irradiating photons. The ratio of the number of desorbed molecules to the irradiated photon number is called the photo-desorption coefficient. The magnitude of this coefficient depends on the surface condition of a duct material, and decreases with the integrated photon dose (scrubbing). The main components of the desorbed gas are  $H_2$ ,  $CO$ , and  $CO_2$ . The relative amount of these molecules depends on the surface composition. Generally, an extruded surface shows a large photo-desorption coefficient and an oxide layer on the extruded surface contains a large amount of carbon compositions, which are released as  $CO$  and  $CO_2$  under the irradiation of synchrotron radiation. Since getters are used as the main pump, the reduction of the photo-desorption coefficient is important to avoid frequent conditioning of the getters and to keep their life long. To reduce the photo-desorption coefficient, chemical cleaning is applied. The first oxide layer on the extruded surface is removed chemically and a new oxide layer with much less carbon is formed. By chemical cleaning, the relative amount of desorption of  $CO$  and  $CO_2$  is reduced as well as the total amount of desorption. The cleaning procedure which was developed by NEOS Co. Ltd. for KEKB, consists of four important steps:

- (1) Degreasing  
 $Na_3PO_4$  3% + NEOS Newclear #100 (a surfactant) 1% 40–45°C for more than 2 h.
- (2) Chemical polishing  
 $H_2SO_4$  0.5–2.0% +  $H_2O_2$  1.0–3.0% + isopropanol 0.2–0.7% + water (rest) typically at 23°C for 15 min.
- (3) Spray washing with deionized water.
- (4) Drying with spurting boil-off  $N_2$  gas.

The removed surface is 1–2  $\mu m$  thick. Fig. 1 shows the difference of the AES depth profile between before and after cleaning. It has been found that this cleaning is also effective to reduce the secondary electron emission coefficient [6].

## 2.3. Structures related to impedance

The inside of a beam duct is designed to be as smooth as possible. The only bump in a duct is a photon mask that makes a shadow for a downstream bellows unit and flanges. The use of the standard Conflat flange for connecting the beam duct leaves a gap between the flanges, where beam-induced fields just below the cut-off frequency can be trapped. To avoid this gap, Helicoflex-delta (Le Carbone K.K) with the same inner diameter as a beam duct is adopted. Except for the HER bend chamber and gate valves with a racetrack aperture, the Helicoflex-delta plays a double role of a vacuum seal and an RF bridge.

For the HER the Helicoflex is not circular, but of a racetrack. For this Helicoflex, we used a

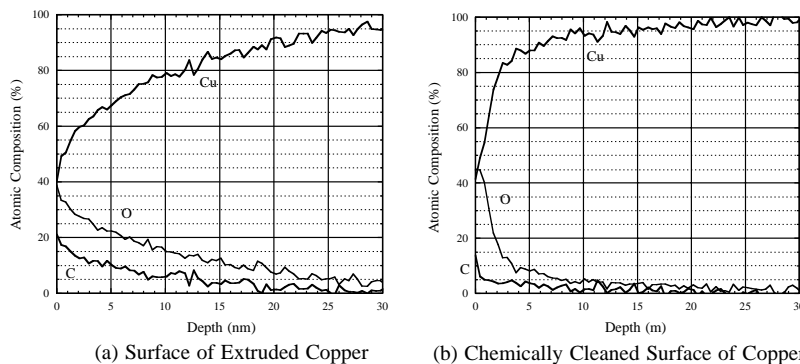


Fig. 1. AES depth profile of a copper surface: (a) extruded surface, and (b) chemically cleaned surface.

circular flange with screw bolts arranged in a circle. This arrangement of screw bolts is not good. Because screws are not distributed uniformly along the Helicoflex, the compressing force along the sealing line is not uniform when screws are tightened with the same torque. In addition, since the distance from a segment of the Helicoflex to the nearest screw varies along the sealing line, the deformation of the flange is not uniform around the Helicoflex. This further enhances the non-uniformity of the compressing force. As a result, a small leak remains. This problem is solved by omitting some screws and adjusting the tightening force of the remaining screws (Fig. 2).

The opening for the pump port is screened with slots which are further backed by crossing bars to reduce the penetration of the TE mode of beam-induced fields, which causes a heat-up of the pumping elements (Fig. 3).

Since more than 2000 bellows units are used in the two rings, special care was taken concerning the reliability of their RF contacts. In our design, contact fingers are pressed by spring fingers to ensure the strength of the contact force between the contact finger and an inner tube (Fig. 4). By



Fig. 3. Shield grid (LER).

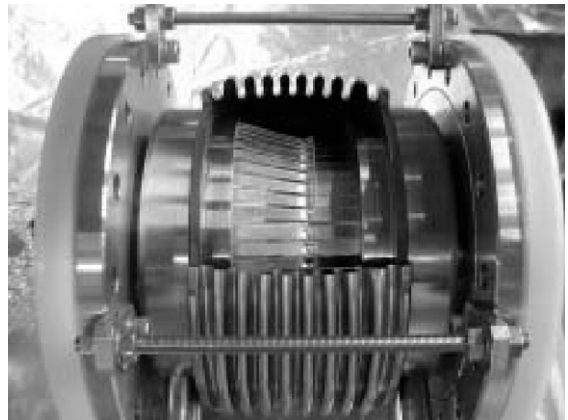


Fig. 4. A cut model of the bellows unit for the LER.

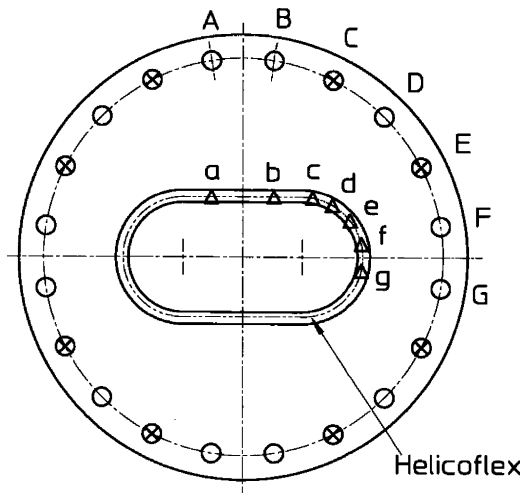


Fig. 2. Screw bolt assembly for HER Flange. Screw bolts at C, E and their equivalent position were omitted. The tightening force of screw bolts at F, G and their opposite position is specified to be half of that for other screw bolts. The positions a–g show the nearest point on the Helicoflex from screw position A–G, respectively.

using the spring finger, the contact force can be guaranteed for an arbitrary shaped inner tube. The contact was tested as a part of a wave-guide up to the same peak wall current density as the design current. Through this test, a contact force of 80–100 g per finger was adopted for the design. The coupling of the coaxial field in the bellows space and the field in the duct through slits between fingers was also studied. The estimated leakage of beam-induced fields was about 6–18 W in power, and was thought to be allowable because the bellows unit is water cooled [7].

For all-metal gate valves, 70 in total, the standard design of VAT Series 47 is adopted. The leakage of fields traveling a duct into the body

through RF bridge is estimated by two methods [8]. One is the same method as that used for the bellows. This measurement gave a power of 10 W as a possible leakage. The other is a calculation using MAFIA for a simplified model of the gate valve. This gave an estimated power of 15–90 W. For a power of 90 W, the temperature of the gate valve reached 200°C if no proper cooling is applied. If this happens, a cooling jacket will be necessary.

#### 2.4. Pumping scheme

The goal pressure to be achieved at KEKB in the presence of the maximum beam current is about  $10^{-9}$  Torr. The pumping speed is designed to realize this pressure when the photo-desorption coefficient is  $10^{-6}$  molecules photon $^{-1}$  [9]. For a chemically cleaned surface according to the procedure described Section 2.2, this value is reached after obtaining an integrated operating current of 1000 A h for both rings. The necessary linear pumping speed is  $100 \ell \text{ s}^{-1} \text{ m}^{-1}$  for each ring. To realize this pumping speed, a pumping port with a net pumping speed of  $100 \ell \text{ s}^{-1}$  at  $10^{-9}$  Torr for a beam duct is prepared at every 1 m. For the HER bending chambers, where a bending magnet leaves no space for pumping ports, a side pump channel is attached. In practice, the ideal distribution of pump ports is not possible because of the presence of magnets. Further, because of the grid which shields a pumping port, the net pumping speed to a beam pipe is less than  $100 \ell \text{ s}^{-1}$ . In the final design, the linear pumping speed is 70 and  $60 \ell \text{ s}^{-1} \text{ m}^{-1}$  for the LER and the HER, respectively.

We have adopted NEG (Non-Evaporable Getter (SAES)) St707 as the main pump. A special module arranged with short NEG strips has been designed for a pump port (Fig. 5). The pumping speed of this assembly for CO is  $200 \ell \text{ s}^{-1}$ . After 0.3 Torr  $\ell$  gas is absorbed, the pumping speed decreases to  $100 \ell \text{ s}^{-1}$ . The lifetime is about 500 Torr  $\ell$ . For a HER bending chamber, four strips ( $2.7 \text{ m} \times 3 \text{ cm}$ ) are inserted in the side channel. In total for the HER and the LER, 2595 pieces of the strip were used. In addition to the NEG, ion pumps which can keep a pumping



Fig. 5. NEG pump.

speed of  $200 \ell \text{ s}^{-1}$  down to  $10^{-10}$  Torr, are installed at every 10 m. A roughing valve is located at every 40 m.

#### 2.5. Monitoring and control

The vacuum system of the ring is controlled from 12 local control stations separately. In each local station, control and interlock signals are managed by a programmable controller. The controllers communicate with each other by optical fibers; thus, local information is reflected to the interlock for the whole ring. Communication between the central control room and the local system is performed based on the formalism of the EPICS system.

An abnormal signal of the component temperature or cooling-water flow activates the beam-abort system. If vacuum pressure shows an abnormal increase, the gate valves around that region are closed. Before closing gate valves, a stored beam must be dumped to avoid any damage to the RF-bridge of the gate valve.

The pressure of the ring is monitored with cold cathode gauges (CCG) at the same pumping port as ion pumps (i.e. every 10 m). With this interval, a leakage can be detected before the effect of the local pressure becomes comparable to the effect of the overall ring pressure (see appendix). Twenty-four extractor gauges are installed, each of which is paired with a CCG to check for any long-term variation of the sensitivity of the CCG. Twenty-four residual gas analyzers (RGA) are also installed. A com-

mercially available RGA is sold with control software, which is usually exclusive. In our case, the RGA is controlled directly using commands based on the RS232C protocol. These commands are delivered from VME, which is controlled by EPICS.

### 3. Manufacturing and installation

Most of copper–copper connections are welded using an electron beam. For the copper stainless-steel transition, explosive bonding or brazing or hot isostatic press (HIP) was selected according to the manufacturer’s choice. Any explosive-bonded material should be machined with care, because stress exerted during the bonding process remains in the material.

The basic manufacturing procedure for a beam duct consists of machining, chemical cleaning, and welding, in that order. After welding, chemical cleaning is avoided considering the possibility that the remnant of chemicals causes corrosion. Since the character of the vacuum surface of a chamber bears its history, great care was taken to keep the surface clean during various fabrication procedures after chemical cleaning. For example, in applying electron beam welding, careful attention is paid to sputtered copper particles and copper vapor during welding. After welding, a purge of the air is waited until the temperature of the material becomes less than 80°C to avoid any unnecessary oxidization of the vacuum surface.

Nearly all chambers were baked before installation to check the thermal outgassing rate and the soundness of the welding [10]. After installation, only ion pumps were baked in situ. Completely oil-free vacuum pumps were used throughout. Fig. 6 shows a recent view of the arc section of the two rings.

### 4. Basic performance

#### 4.1. Pressure

After installation, within one month, the base pressure of most parts of the rings reached the



Fig. 6. Picture of the arc section. The left-hand side is the LER. The right-hand side is the HER.

$10^{-10}$  Torr range. The decrease in the pressure rise per beam current is shown in Fig. 7 for both rings. An estimated photon desorption coefficient is also shown in the figures. The photo-desorption coefficient is slightly higher at a low photon dose than the R&D data for the same chemical cleaning, but decreases almost as expected.

In the case of vacuum work, for example, during the replacement of vacuum chambers, the ring is vented using boil-off nitrogen gas from liquid nitrogen. A new chamber is baked before installation. After the chambers are replaced, rough pumping starts with an oil-free roughing system. Then, only the ion pumps are baked to recover their maximal pumping speed. The next step is the activation of the NEG. After about 6 h from rough pumping, the pressure enters the  $10^{-9}$  Torr range. At this stage, beam injection can be restarted.

The only high outgassing component is a septum magnet, which is set in a vacuum. The outgassing source is an insulation coat on an iron plate. The limited conductance between the septum chamber and the ring vacuum chamber reduces the effect of this high outgassing on the ring pressure. Nevertheless, when the injection efficiency is low, or continuous injection is necessary; a long-time operation of the septum magnet increases the ring pressure considerably and sometimes reduces the beam lifetime. A low outgassing iron plate is now being sought.

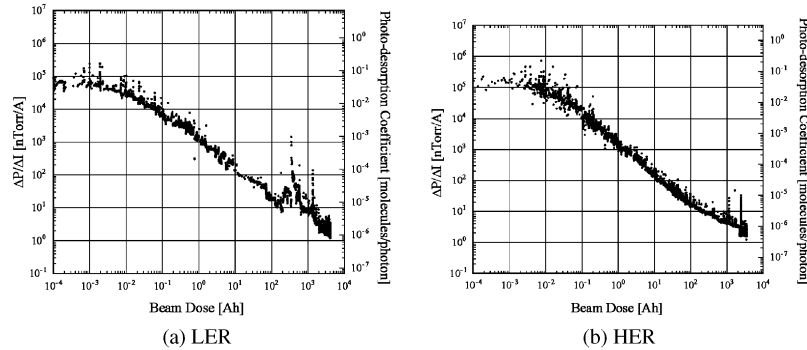


Fig. 7. History of the pressure rise per beam current: (a) average of the LER arc, and (b) average of the HER arc. The pressure reading of CCG is multiplied by a factor of 3 to approximate an actual CO equivalent pressure in the ring. The photo-desorption coefficient is estimated assuming a linear pumping speed of  $30 \ell \text{ s}^{-1} \text{ m}^{-1}$ .

#### 4.2. Temperature of the components

When the beam current is low, no structural heating of the bellows and gate valves was observed. Only some stainless-steel chambers with comparatively small diameters (55–64 mm) were heated by the wall current. These were replaced with copper chambers.

Recent higher current operation has revealed the excitation of a resonant mode inside bellows and a heating up of the bellows unit. This is caused by the TE mode of a beam-induced field, whose longitudinal magnetic field couples through the gap between the contact fingers with a resonant mode inside bellows. This case happens when the cross-section of the vacuum chamber has no center of symmetry, or when the beam orbit is off center. Actually, the heat up of the bellows unit is observed near to the Ver.4 movable masks and abort windows where the cross-section of the beam pipe is not symmetrical with respect to the beam orbit. The temperature rise is not critical at present. Cooling by a fan from outside is effective. However, constant monitoring is necessary.

### 5. Special phenomena associated with the beam

#### 5.1. Electron cloud

At every CCG of the LER and the HER, which is located at a pumping port close to the down-

stream end of a bending magnet, a false indication of pressure due to photoelectrons was observed. This gives an apparent pressure that is linearly dependent on the beam current, but the slope never decreases with increasing beam dose. For our CCG, pressure is given by the discharge current as  $P \sim I_{\text{dis}}^{0.95}$ . This means that the stray electron are proportional to the beam current, like  $I_e \sim I_{\text{beam}}^{1.05}$ . By attaching a small dipole magnet at the neck of the gauge port, these electrons were steered and the reading of CCG became normal.

In the LER, a non-linear dependence of the pressure on the beam current is observed. At a location where strong synchrotron radiation hit a chamber wall, this non-linearity overlaps the linear dependence of the photon desorption on the beam current, and not very obvious. Where no synchrotron radiation exists, strong non-linearity is observed (Fig. 8). This is understood as electron multipactoring, [11]; their dependence on the bunch pattern is well explained by this model [12].

In the LER the electron-cloud instability causes a beam blow-up. The cloud consists of photoelectrons and multiplied electrons by multipactoring. The above-mentioned pressure anomaly is thought to be caused by the electron cloud. To obtain direct information of the electron cloud in the beam duct, electron detectors were installed at a pumping port near a bending magnet. Fig. 9 shows the result of a DC measurement. The non-linearity of an electron current with respect to the beam current is understood to imply the combined

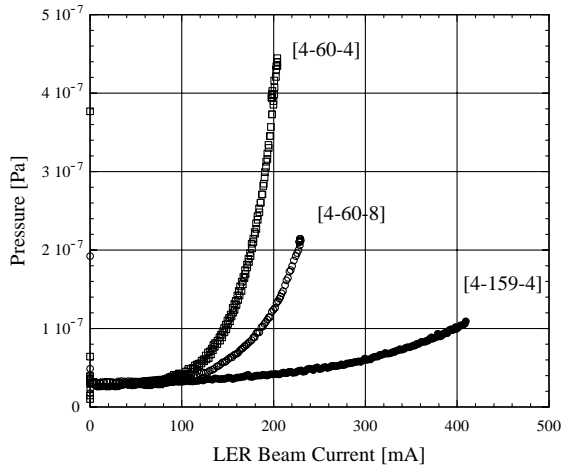


Fig. 8. Non-linear pressure variation observed in the LER vacuum chamber at IR. The numbers in the square brackets indicate a bunch pattern as [No. of trains, No. of bunches in a train, Bunch spacing]. The behavior depends on the bunch pattern.

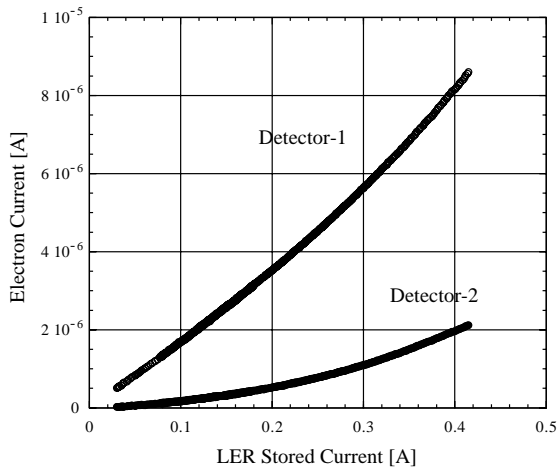


Fig. 9. Electron current measured in the arc section of the LER. Detector-1 is located at a pump port 1.8 m downstream from the center of a bending magnet. Detector-2 is 8.6 m downstream from the center of the bending magnet.

contribution of photo-electrons and multipacted electrons. The difference of the electron current between the detector-1 and the detector-2 is mainly due to the difference of the intensity of synchrotron radiation at each location. However, the ratio of the electron current of the detector-2 to that of the detector-1 is larger than the ratio of the

intensity of synchrotron radiation at their location. The electron current of the detector-2 is contributed dominantly by the multipactoring process. A fast measurement shows that the observed current is associated with each train, and is proportional to the average beam density within the train. The build up and the decay of the electron current occur within  $0.5 \mu\text{s}$ , including the time constant of the measurement system. At present a fast measurement is possible only where synchrotron radiation is strong.

## 5.2. Damage by beam

Since the transverse dimension of the bunch is quite small, vacuum chambers are exposed to the danger of direct damage by the beam. Even if the length of the material is shorter than its radiation length, and therefore a very small amount of energy is deposited through the ionization process (about 170 J for 1 cm copper by a 1 A beam), if nearly the total charge of the design current hits the material, the path of the beam will melt away. If the length of the material is longer than the radiation length, even a fraction of the total current will melt the material by the energy deposited from the electro-magnetic shower. The latter case is seen in movable masks. To avoid the accident due to an unstable transient behavior of the beam, a fast abort system has been tried, but is not effective at present.

When the need to clear a stored beam arises, the beam must be carefully extracted from the ring and be absorbed locally to avoid any damage to the vacuum chamber or component and not to increase the radiation level in the tunnel. This extraction window is made of Ti with 1 mm thickness. The window is inclined by  $45^\circ$  to an outgoing beam. Recently, it was found that about a 1 A positron beam passing close to a Helicoflex seal (Al lining) in front of a window makes a hollow on the sealing surface of the Helicoflex and causes a vacuum leak. According to an analogy of a two-dimensional calculation of a static electric field, when the beam approaches a (circular) duct wall at distance  $d$ , the wall current density at the nearest surface increases as  $d^{-1}$ , and within  $2d$  of the circumference, half of the total wall current is



confined. This fact can be a cause of this damage. However, no detailed explanation has yet been given.

## 6. Summary

Two electron and positron storage rings with a circumference of 3016 m were constructed using copper vacuum chambers. The structures used to minimize the effect of beam-induced fields, such as RF contacts in gate valves and bellows, and Helicoflex seals in flanges, are working successfully for the most part. However, with increasing current, the effect of the TE mode created by singular chambers on bellows heating became apparent. A special procedure of chemical polishing was developed to clean an extruded surface of copper for the KEKB vacuum chamber. The resulting surface is quite stable and clean. The photon desorption coefficient is decreasing almost as expected. Especially in the LER, some phenomena related to an electron cloud in a beam duct have been observed. At a higher current, direct damage by the beam is a serious problem.

## Acknowledgements

The design of the KEKB vacuum system was possible by learning from various experiences on accelerator vacuum from many laboratories around the world. First, we would like to thank those researchers who lead us on various occasions. In addition, sincere thanks are due to the member of the accelerator department of KEKB for their collaboration from construction to commissioning. Also, to realize a vacuum system with the designed property, invaluable efforts were put into manufacturing and installation by many companies. We send our heartfelt thanks to them.

## Appendix

The pressure distribution due to a local leakage is expressed as

$$P(x) = P_0 e^{-(|x|/\lambda)},$$

where  $P_0$  is the pressure at the leak point,  $x$  is the distance from the leak point, and  $\lambda$  is given by

$$\lambda = (\text{conductance of the unit length of beam duct/linear pumping speed})^{1/2}.$$

The conductance of a 1 m long beam duct is 102 and  $52.3 \ell \text{ s}^{-1}$  for the LER and the HER, respectively. Therefore,  $\lambda$  is 1.2 and 0.9 m for each ring, and roughly 1 m for both rings. If the leak point is at the middle of the gauge separation ( $x = 5$ ),  $P_0$  which is higher than  $P_{\text{av}} \times e^{5/\lambda} \approx 150P_{\text{av}}$  ( $P_{\text{av}}$  is the average pressure of the ring) is detectable. The effect of this local leak is proportional to

$$\int_{-\infty}^{\infty} P_0 e^{-|x|/\lambda} dx = 2\lambda P_0.$$

$2\lambda P_0$ , is equal to  $300P_{\text{av}}$  in this case. On the other hand, the effect of the whole ring is proportional to  $C \times P_{\text{av}}$ , where  $C$  is the circumference, and equals to 3016 m. Accordingly, with a gauge interval of 10 m, any leakage can be detected before the effect of the local pressure becomes comparable to that of the overall ring pressure.

## References

- [1] H. Hisamatsu, H. Ishimaru, K. Kanazawa, S. Kato, M. Nakagawa, M. Sato, M. Shimamoto, Y. Suetsugu, N. Terunuma, *Vacuum* 47 (1996) 601.
- [2] K. Kanazawa, S. Kato, Y. Suetsugu, H. Hisamatsu, M. Shimamoto, M. Sato, M. Shirai, *Appl. Surf. Sci.* 169 (2001) 715.
- [3] R. Ballion, J. Boster, W. Giesske, H. Hartwig, D. Jagnow, R. Kose, J. Kouptsidis, G. Schumann, M. Schwartz, *Vacuum* 41 (1990) 1887.
- [4] Y. Namito (KEK), unpublished.
- [5] Y. Nagai (Hitachi Cable), unpublished.
- [6] S. Kato, K. Kanazawa, N. Kitano, N. Matsuda, 45th AVS International Symposium, Baltimore, 2–6 November, 1998.
- [7] Y. Suetsugu, K. Ohsima, K. Kanazawa, *Rev. Sci. Instrum.* 67 (1996) 2796.
- [8] Y. Suetsugu (KEK), unpublished.
- [9] Y. Hori, M. Kobayashi, Y. Takiyama, *J. Vac. Sci. Technol. A* 12 (1994) 1644.
- [10] K. Kanazawa, S. Kato, Y. Suetsugu, H. Hisamatsu, M. Shimamoto, M. Sato, M. Shirai, *Appl. Surf. Sci.* 169 (2001) 720.
- [11] O. Gröbner, 10th International Conference on High Energy Accelerators, Protvino, July, 1977.
- [12] Y. Suetsugu, 2001 Particle Accelerator Conference, Chicago, 18–22 June, 2001.